J|A|C|S
ARTICLES
Published on Web 04/05/2003

Evaluation of Multivalent Dendrimers Based on Melamine: Kinetics of Thiol−Disulfide Exchange Depends on the Structure of the Dendrimer

Wen Zhang, Shane E. Tichy, Lisa M. Pérez, Gheorghe C. Maria,[†,‡]
Paul A. Lindahl, and Eric E. Simanek*

Contribution from the Department of Chemistry, Texas A&M University, College Station, Texas 77843, and Laboratory of Chemical and Biochemical Reaction Engineering, University Politechnica, Bucharest, Romania

Received August 15, 2002; E-mail: simanek@tamu.edu

Abstract: The rate of thiol−disulfide exchange of dansyl groups mediated by dithiothreitol depends on the structure of the dendrimer. In general, the rate of exchange decreases as the size of the dendrimer increases. Dendrimers with disulfides attached near the core undergo exchange more slowly than dendrimers with disulfides near the periphery. Exchange is a bimolecular (noncooperative) process between dansyl-linked disulfides and dithiothreitol. No evidence for intramolecular macrocylization (cooperative) exchange is observed. Mass spectrometry is used to follow exchange in two dendrimers, providing qualitative and quantitative information about this process. Mathematical models suggest that the rates for exchange for all disulfides of a dendrimer are similar, but increase as the exchange reaction progresses.

Introduction

Thiol−disulfide exchange offers both a convenient method for the attachment of ligands to multivalent macromolecules and an opportunity to exploit "programmable release" of these ligands upon exposure to a reducing environment. Accordingly, disulfides have been employed to conjugate small molecules to soluble scaffolds including proteins and synthetic polymers for drug delivery.[1−3] These disulfides are biolabile. Thiols including glutathione, cysteine, and homocysteine appear in human plasma at low concentrations, 10, 5, >1 μM, respectively, while intracellular concentrations of these reducing agents are significantly (>100×) higher.[4−6] Here, we explore whether the globular nature of dendrimers offers an opportunity to manipulate the kinetics of thiol−disulfide exchange through the placement of the disulfides within the globular architecture. This manipulation is facilitated by control over atomic connectivity, and not by any ability to exercise precise control over the shape of these macromolecules in three dimensions. Here, we describe five dendrimers, **1**−**5**, that differ in size, valency, and placement of disulfide-linked dansyl groups (Chart 1). Dansyl groups were chosen as models of drugs because they offer a convenient spectrophotometric probe for monitoring the kinetics of exchange processes and are sufficiently hydrophobic so that a rapid extraction step could be used to quantify the extent of exchange.

The globular nature of the dendrimer provides a high density of disulfide groups that in the presence of a *single* molecule of glutathione (GSH) or other endogenous thiol could undergo thiol−disulfide exchange to rapidly shed *all* ligands of interest from the dendrimer. Such an event could be beneficial for drug delivery applications. One pathway for this process (Scheme 1) arises from phase partitioning and local concentration effects. The covalent architecture is shown with solid lines and the hydrophobic environment (dendritic phase) with a dotted circle to distinguish it from bulk solution. While not described here, we envision that thiol−disulfide exchange reactions could be used to replace a group, RS (i.e., thiopyridine), with the ligands, LSH, of interest.[7] When this conjugate is introduced to physiological conditions, a single molecule of glutathione, GSH, could mediate thiol−disulfide exchange, leading to a free thiol on the dendrimer. Intramolecular reaction of this thiol to form the macrocycle releases a second ligand LSH. If the ligand is hydrophobic and preferentially partitions in the dendrimer phase instead of water, further reaction can take place until all ligands are released as shown. The formation of the dendritic poly(macrocycle) could further alter the hydrophobic environment leading, to changes in the rates of exchange.

A number of observations suggested that the cooperative pathway described by Scheme 1 might be accessible. First, there are many reports of sequestration of hydrophobic molecules by

[†] University Politechnica.

[‡] Current address: Department of Chemistry, Texas A&M University, College Station TX 77843.

(1) Huang S. Y.; Pooyan S.; Wang J.; Choudhury I.; Leibowitz M. J.; Stein S. *Bioconjugate Chem.* **1998**, *9*, 612−617.
(2) Trimble, S. P.; Marquardt, D.; Anderson, D. C. *Bioconjugate Chem.* **1997**, *8*, 416−423.
(3) Trail, P. A.; Willner. D.; Knipe., J.; Henderson, A. J.; Lasch, S. J.; Zoeckler, M. E.; Trailsmith, M. D.; Doyle, T. W.; King, H. D.; Casazza, A. M.; Braslawsky, G. R.; Brown, J.; Hofstread, S. J.; Greenfiled, R. S.; Firestone, R. A.; Mosure, K.; Kadow, K. F.; Yang, M. B.; Hellstroem, K. R.; Hellstroem, I. *Cancer Res.* **1997**, *57*, 100−105.
(4) Araki, A.; Sako, Y. *J. Chromatogr.* **1987**, *422*, 43−52.
(5) Burgunder, J. M.; Nelles, J.; Bilzer, M.; Lauterburg, B. H. *Eur. J. Clin. Invest.* **1988**, *18*, 420−424.
(6) Meister, A. *Pharmacol. Ther.* **1991**, *51*, 155−194.

(7) By using dendrimers displaying thiopyridine groups, both captopril and cysteine-containing peptides can be incorporated onto dendrimers. Umali, A.; Simanek, E. E. *Org. Lett.* **2003**. In press.

10.1021/ja0210906 CCC: $25.00

Chart 1

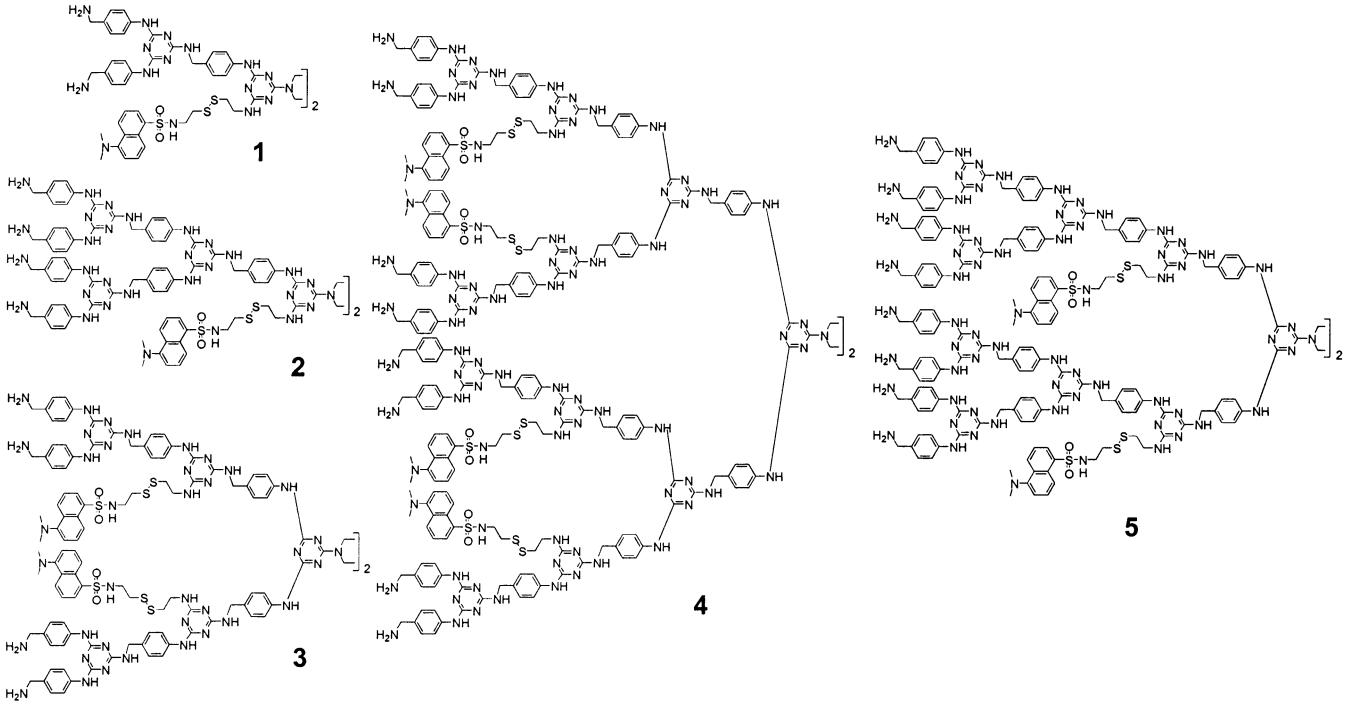

Scheme 1. Hypothetical Reaction with Glutathione (GSH) Can Mediate Exchange through Bimolecular or Cooperative Processes[a]

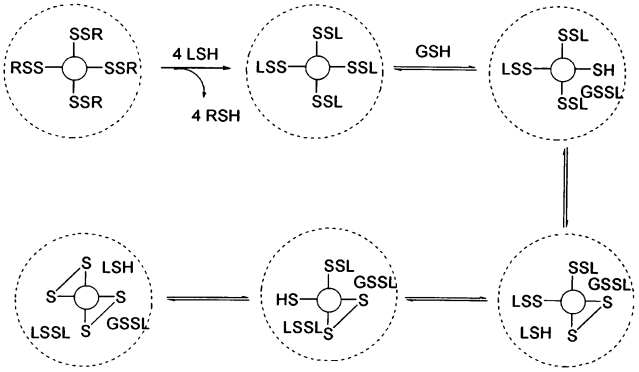

[a] Dotted line represents the dendritic phase. The multivalent scaffold can be prepared by exchange groups (RS) with ligands (LS) of interest.

dendrimers.[8−18] Most notable is Meijer's "dendritic box" which sequesters hydrophobic guests as a function of the peripheral group.[16−18] Such sequestration in our system could lead to cooperative release of ligands from the dendrimer. Second, intramolecular thiol−disulfide exchange to form large macrocycles has been reported.[19−22] Notably, Rabenstein has observed that the single disulfide of somatostatin (RSSR),which has undergone thiol−disulfide exchange with glutathione (GSH) to yield the mixed thiol−disulfide, reacts intramolecularly to form a 38-atom macrocycle faster than intermolercularly with a second equivalent of glutathione.[19] Arginine vasopressin and oxytocin follow similar trends, forming 20-membered rings.[20,21] Zhang and Snyder have reported on the cyclization of dipeptides containing two cysteine residues separated by up to five amino acids mediated by oxidized glutathione.[22] Third, the mechanism for thiol−disulfide exchange has been investigated and involves the S_N2 reaction of thiol or the more reactive thiolate anion.[23−25] Given that our dendrimers comprise basic triazines, opportunities for thiolate generation or enhanced nucleophilicity of the thiols is also possible.

Dithiothreitol (DTT) was chosen to mediate exchange instead of glutathione to simplify analysis. While glutathione is physiologically relevant and introduces interesting questions including the role of charge and additional steric bulk on thiol−disulfide exchange, its use complicates interpretation of data resulting from the transient formation of dendrimer−glutathione mixed disulfides. These complications lead us to save such inquiries for other studies of advanced architectures with established biocompatibility.[26] However, equilibrium constants between GSH/DTT redox pairs have been determined.[27]

(8) Newkome, G. R. Moorefield, C. N.; Baker, G. R.; Johnson, A. L.; Behera, R. K. *Angew. Chem., Int. Ed. Engl.* **1991**, *30*, 1176−1178.
(9) Newkome, G. R.; Moorefield, C. N.; Baker, G. R.; Saunders, M. J.; Grossman, S. H. *Angew. Chem., Int. Ed. Engl.* **1991**, *30*, 1178−1180.
(10) Hawker, C. J.; Wooley, K. L.; Fréchet, J. M. J. *J. Chem. Soc., Perkin Trans. 1* **1993**, 1287−1297.
(11) Liu, M.; Kono, K.; Fréchet, J. M. J. *J. Controlled Release* **2000**, *65*, 121−131.
(12) Pistolis, G.; Malliaris, A.; Paleos, C. M.; Tsiourvas, D. *Langmuir* **1997**, *13*, 5870−5875.
(13) Pistolis, G.; Malliaris, A.; Tsiourvas, D.; Paleos, C. M. *Chem.-Eur. J.* **1999**, *5*, 1440−1444.
(14) Heise, A.; Hedrick, J. L.; Frank, C. W.; Miller, R. D. *J. Am. Chem. Soc.* **1999**, *121*, 8647−8648.
(15) Jansen, J. F. G. A.; Peerlings, H. W. I.; Van Hest, J. C. M.; Meijer, E. W.; De Brabander van den Berg, E. M. M. NATO Advanced Study Institute Series C; Plenum: New York, 1997; Vol. 499, pp 371−384.
(16) Jansen, J. F. G. A.; de Brabander van den Berg, E. M. M.; Meijer, E. W. *Science* **1994**, 266, 1226−1229.
(17) Jansen, J. F. G. A.; Meijer, E. W.; de Brabander-van den Berg, E. M. M. *J. Am. Chem. Soc.* **1995**, *117*, 4417−4418.
(18) Zhang, X.; Wilhelm, M.; Klein, J.; Pfaadt, M.; Meijer, E. W. *Langmuir* **2000**, *16*, 3884−3892.
(19) Rabenstein, D. L.; Weaver, K. H. *J. Org. Chem.* **1996**, *61*, 7391−7397.
(20) Rabenstein, D. L.; Yeo, P. L. *J. Org. Chem.* **1994**, *59*, 4223−4229.
(21) Rabenstein, D. L.; Yeo, P. L. *Bioorg. Chem.* **1995**, *23*, 109−118.
(22) Zhang, R.; Snyder, G. H. *J. Biol. Chem.* **1989**, *264*, 18472−18479.
(23) Wilson, J. M.; Bayer, R. J.; Hupe, D. J. *J. Am. Chem. Soc.* **1977**, *99*, 7922−7926.
(24) Szajewski, R. P.; Whitesides, G. M. *J. Am. Chem. Soc.* **1980**, *102*, 2011−2026.
(25) Houk, J.; Whitesides, G. M. *J. Am. Chem. Soc.* **1987**, *109*, 6825−6836.

Table 1. Molecular Weight Data for **1**−**5** and Protected Precursors Including MALDI-TOF, Dynamic Light Scattering (DLS), and Size Exclusion Chromatography (SEC) (the structures of the Protected Dendrimers (**8**, **11**, **14**, **17**, **20**) are given in Supporting Information)

deprotected		protected			
dendrimers	MALDI	dendrimers	MALDI calc, (obsd)	DLS	SEC
1	1891.62 (1890.40)	**8**	2290.83 (2290.86)	2.50 kDa 2.36 nm	M_n 2217, M_w 2290, M_w/M_n 1.03
2	3167.98 (3167.85)	**11**	3968.78 (3968.20)	4.22 kDa 3.18 nm	M_n 3724, M_w 3766, M_w/M_n 1.01
3	4333.85 (4333.39)	**14**	5134.43 (5133.57)	5.52 kDa 3.70 nm	M_n 4255, M_w 4335, M_w/M_n 1.02
4	9219.61 (9219.12)	**17**	10824.03 (10820.91)	12.70 kDa 5.90 nm	M_n 6055, M_w 6268, M_w/M_n 1.03
5	6887.80 (6888.30)	**20**	8526.24 (8490.15)	9.35 kDa 4.98 nm	M_n 5369. M_w 5572, M_w/M_n 1.03

Experimental Section

Release Studies. Thiol−disulfide exchange was monitored in 20 mM phosphate buffer at pH 7.5. To perform a single exchange experiment, multiple (10−15) reaction vials were prepared containing degassed buffer. Dendrimer was added to each from a stock solution. Upon addition of DTT (from a stock solution) to each reaction vial, the vials were placed on a shaker table to ensure adequate mixing to reduce artifacts arising from mass transport. At a given time, a vial was removed from the shaker plate. One milliliter of chloroform was added and the mixture shaken to extract the chromophore. Molecules **1**−**5** are soluble in water and only sparingly soluble in chloroform over almost the entire concentration range of these solutions. The phases were separated with the aide of a quick centrifugation step. An aliquot (0.5 mL) of the organic phase was removed via syringe, and the fluorescence of the resulting solution was determined. Mass spectral analysis of the organic phase revealed no disulfides of the dansyl chromophore, only free thiols. Addition of acetic acid to quench the reaction did not appear to affect the measurement. Analyses were performed in duplicate to estimate the magnitude of experimental error.

Fluorescence Quantification. Fluorescence spectra were recorded on an SLM Instruments AMINCO spectrophotometer using an excitation wavelength of 350 nm and monitoring emission at a wavelength of 497 nm.

Mass Spectrometry Studies. Matrix-assisted laser desorption/ionization time-of-flight (MALDI-TOF) spectra were recorded in linear ion mode with an Applied Biosystems Voyager DE-STR mass spectrometer (ABI, Framingham, MA). Positive ions were generated by using a nitrogen laser pulse ($\lambda = 337$ nm, 20 Hz) and accelerated under 20 kV using delayed extraction (550 ns) before entering the time-of-fight mass spectrometer. Laser strength was adjusted to provide minimal fragmentation and optimal signal-to-noise ratio. An average of 200 laser shots was used for each spectrum, and data were processed with the accompanying Voyager software package.

The exchange reactions were performed at approximately pH 4.5 to retard the rates of reaction so that more data could be collected early in the time course and errors that could result from delays in workup or data acquisition could be avoided. An overlayer preparation which has been described previously was used with 2,4,6-trihydroxyacetophenone (THAP).[28] A 1:1 mixture of the 1 μM dendrimer DTT solution and 10 mg/mL THAP solution in methanol was spotted in 1 μL aliquots on top of a 100 mg/mL THAP bed of matrix.[29]

The experimental conditions were optimized prior to the addition of DTT and held constant throughout the monitoring of the experiment. The MALDI mass spectra for **1**−**5** are straightforward to interpret. For example, the mass spectrum of **3** shows peaks at *m*/*z* 4334.74, 4356.84, and 4372.64 attributed to protonated, sodiated, and potassiated molecules, respectively. Fragment ions at 4316.43 and 4299.37 were also observed. The total analyte response was taken to be the total area of these five peaks. The areas of peaks of interest were calculated using the automatic integration function included with the Voyager (Data Explorer) software package.[30]

Kinetic Modeling. Models were developed to fit the observed kinetic data from a minimalist approach. Reaction order for dendrimer and DTT were determined experimentally for **3** and **5**. To compare the statistical model with the experimental data, a standard deviation of $\sigma = 3.4 \times 10^{-4}$ mM was used, corresponding to 1% of the initial concentration of dendrimer **3**.[31] The computational strategy used to identify the rate constants of these kinetic models has been described for similar isothermal batch processes.[32,33] Models used initial concentrations identical to those used experimentally and were solved by numerical integration of differential mass balances under constant system−volume conditions. All calculations were done in Matlab (2001) on a Dell PC.[34] Details are available in the Supporting Information.

Structural Modeling of Dendrimers. Computational models were obtained using the Cerius^2 4.6 suite of programs from Accelyrs, Inc. Minimization and dynamics calculations were performed in the gas phase with the open force field (OFF) program using the pcff second-generation force field.[35] The dendrimers were initially drawn and minimized in the fully extended, open conformation before constant volume and temperature (NVT) molecular dynamics calculations were performed using simulated annealing. The simulation annealing was carried out for 840 ps over a temperature range of 300−1000 K, with $\Delta T = 50$ K, using the Nose temperature thermostat, a relaxation time of 0.1 ps, and a time step of 0.001 ps. The dendrimer was minimized after each anneal cycle, resulting in 300 minimized energy structures.

Synthesis. Intermediates and targets provided satisfactory ^{1}H and ^{13}C NMR spectra and mass spectra. The synthesis of related molecules has been described.[36] The syntheses of **1**−**5** are fully described and elaborated upon in the Supporting Information.

Results and Discussion

Evaluation of Molecular Weights. The molecular weights of targets **1**−**5** and the corresponding protected precursors were measured by MALDI-TOF mass spectrometry and are in excellent agreement with expected values (Table 1). The protected precursors were also evaluated by dynamic light scattering and size exclusion chromatography. A strong correlation between all these techniques for the smaller dendritic

(26) Preliminary investigations have shown that triazine dendrimers do not show any changes to liver or kidney function when administered to mice in single bolus injections up to 10 mg/kg. Zhang,W.; Jiang, J.; Qin, C.; Perez, L. M.; Parrish, A. R.; Safe, S. H.; Simanek, E. E. *Supramol. Chem.* **2003**. In press.
(27) Rothwarf, D. M.; Scheraga, H. A. *Proc. Natl. Acad. Sci. U.S.A.* **1992**, *89*, 7944−7948.
(28) Amm, M.; Platzer, N.; Bouchet, J. P.; Volland, J. P. *Magn. Reson. Chem.* **2001**, *39*, 77−84.
(29) Zhou, L.; Russell, D. R.; Zhao, M.; Crooks, R. M. *Macromolecules* **2001**, *34*, 3567−3573.
(30) Koomen, J. M.; Russell, W. K.; Hettick, J. M.; Russell, D. H. *Anal. Chem.* **2000**, *72*, 3860−3866.
(31) To simplify the estimate statistical tests, a normal experimental noise with a minimum level of $\tilde{\sigma} = 3.4 \times 10^{-4}$ mM was considered from experiments and for all the observed species (see Appendix A of the Supporting Information).
(32) Maria, G.; Rippin, D. W. T. *Comput. Chem. Eng.* **1997**, *21*, 1169−1190.
(33) Froment, G. F.; Hosten, L. H. Catalytic Kinetics: Modelling. In *Catalysis: Science and Technology*; Anderson, L., Boudart, M., Eds.; Springer-Verlag: Berlin, 1981.
(34) Matlab 2001. *The Language of Technical Computing*, version 6.1, release 12.1; The MathWorks Inc.: Natick, MA.
(35) *Cerius^2 Force field Based Simulations*, September 1998; Accelerys, Inc.: San Diego, 2000.
(36) Zhang, W.; Nowlan, D. T., III; Thomson, L. M.; Lackowski, W. M.; Simanek, E. E. *J. Am. Chem. Soc.* **2001**, *123*, 8914−8922.

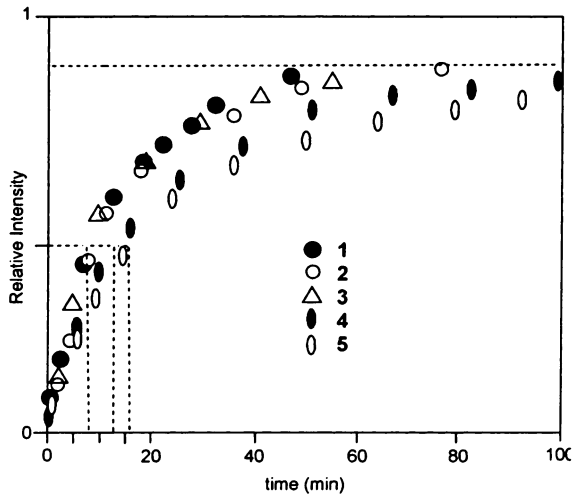

Figure 1. Half-lives for exchange under psuedo-first-order conditions at identical concentrations of dansyl groups. Dendrimers **1**−**3** undergo exchange at similar rates that are 1.8× slower than dendrimer **4** and 2.2× slower than **5**.

molecules **1**, **2**, and **3** is observed. For molecules **4** and **5**, dynamic light scattering is a better predictor of molecular weight than size exclusion chromatography (SEC) which uses polystyrene as a standard. However, SEC reveals an excellent agreement between weight average and number average molecular weights and, as with previous targets, low measured polydispersities. SEC consistently underestimates the molecular weights of the fourth-generation dendrimers by 40%, an observation borne out in other dendrimer architectures as well.[37] The smaller measured hydrodynamic volume when compared with linear poly(styrene) is attributed to the more compact shape of the dendritic architecture.[38] This discrepancy is a "dendritic effect" and suggests to us that if differences in release rates result from the dendritic nature of these architectures, such effects should be pronounced for **4** and **5**, whereas similar *small molecule-like* behaviors should be predicted for **1**, **2**, and **3**.

Determination of Reaction Order

Half-Lives under Pseudo-First-Order Conditions. To determine the order of the reaction, we performed analyses of thiol−disulfide exchange using fluorimetry under pseudo-first-order conditions with an excess of DTT (Figure 1). Our initial assumptions were that no cooperative effects would be observed and, instead, the disulfide-linked dansyl groups of a single dendrimer could be treated as independent molecules. The experimental reproducibility of the exchange processes can be evaluated by comparing the half-lives of the reaction in experiments when the concentration of the dendrimer is varied. That is, the pseudo-first-order assumption can be checked if the half-life is independent of dendrimer concentration as revealed by eq 1.

$$t_{1/2} = \frac{1}{k}\ln\frac{C_o}{C} = \frac{1}{k}\ln 2 \qquad (1)$$

We find excellent internal agreement for half-lives of release for each of the targets **1**−**5** over a range of concentrations (Table 2), suggesting that the reaction is first-order in [dansyl]. One

Table 2. Exchange under Psuedo-First Order Conditions

dendrimer	1		2		3		4		5	
[dendrimer] (μM)	70	7.0	70	7.0	35	3.5	17.5	1.75	35	3.5
[dansyl] (μM)	140	14	140	14	140	14	140	14	140	14
[DTT] (μM)	370	370	370	370	370	370	370	370	370	370
$t_{1/2}$ (min)	7.1	7.4	7.5	7.4	7.3	8.0	14	13	17	16

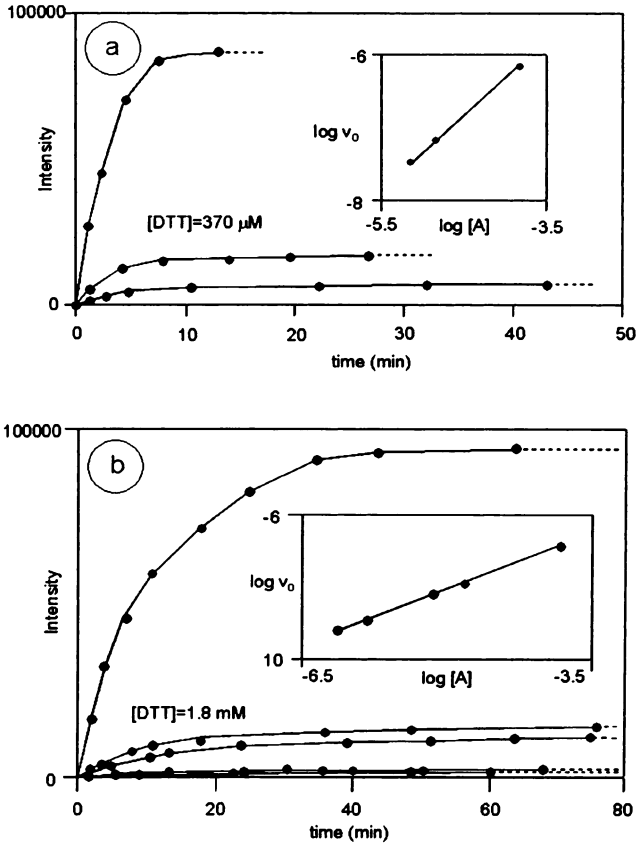

Figure 2. Kinetics of release for **3**. (a) At 1.8 mM DTT, reaction progress was monitored at 7.5, 15, and 150 μM **3**. (b) At 370 μM DTT, reaction progress was monitored at 0.75, 1.5, 7.5, 15, and 150 μM **3**.

of the most interesting conclusions from this work is that comparisons of the half-lives for compounds **1**−**5** indicate that structure *does impact* the kinetics of release. Table 2 shows the results of the loss of dansyl groups from **1**−**5** when under identical concentrations of danysl and DTT. Targets **1**, **2**, and **3** undergo thiol−disulfide exchange at similar rates. These rates are 1.8× faster than the rate of exchange for **4** and 2.2× as fast for **5**. These observations are consistent with the onset of "dendritic character" as seen by SEC.

Method of Initial Rates. We focused further attention on dendrimers **3** and **5**, architectures representative for the series. Analysis of the initial rates of the reactions performed under different concentrations of either dansyl or DTT establishes that the reaction is first-order in both [dansyl] and [DTT]. Representative data of **3** are given in Figure 2 in which the concentration of DTT is held constant in two separate experiments (2a and 2b) and the [dansyl] is varied. The insets show the linear relationship of the logarithms of the initial rates versus the logarithm of initial concentrations. For both lines the slope = 1. Starting with the assumed first-order rate eq 2, we can define an initial rate (rate_o, eq 3) and take the logarithm (eq 4) to reveal that the resulting plot should produce a straight line

(37) Hawker, C. J.; Frechet, J. M. J. *J. Am. Chem. Soc.* **1990**, *112*, 7638−7647.
(38) Aharoni, S. M.; Crosby, C. R.; Walsh, E. K. *Macromolecules* **1982**, *15*, 1093−1048.

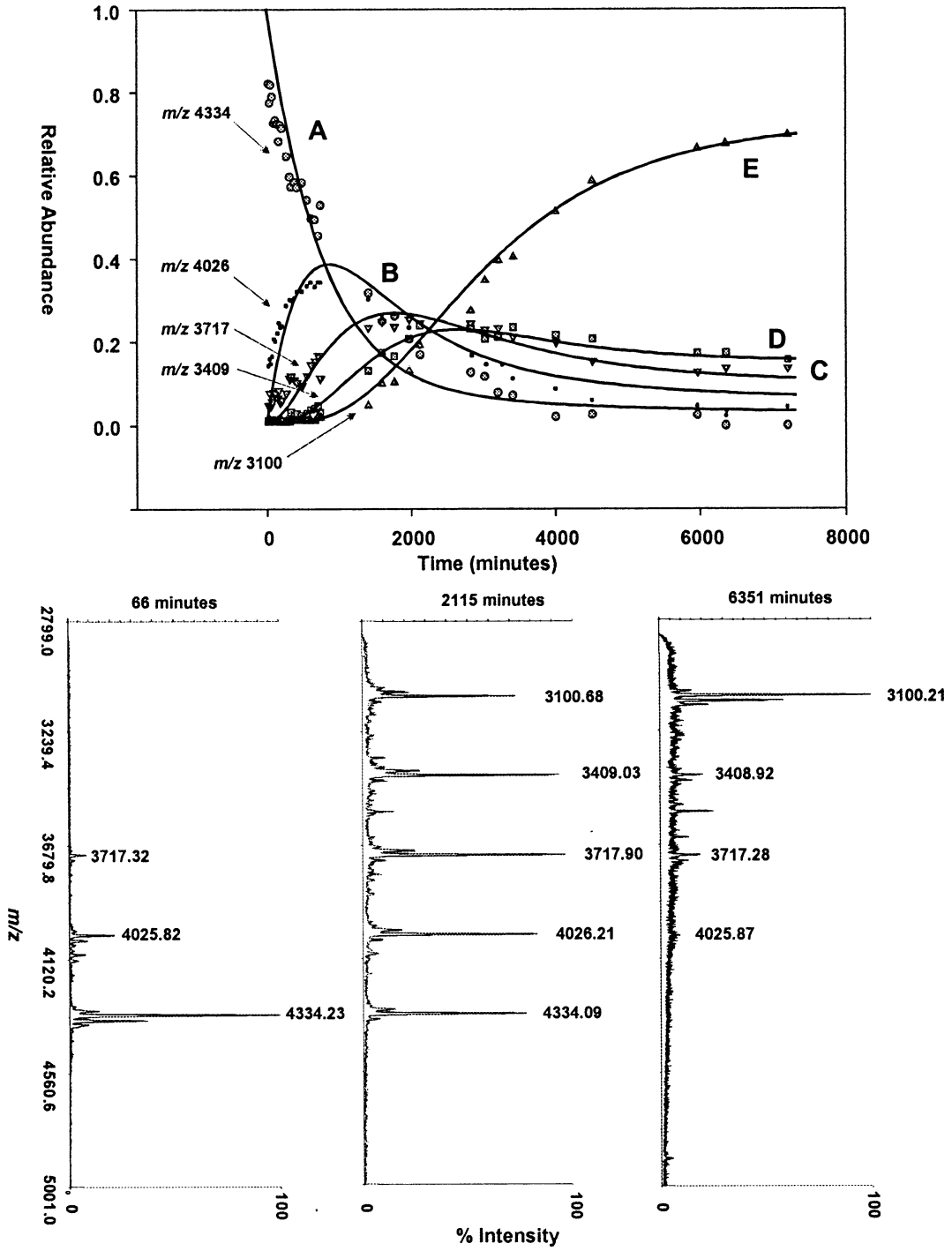

Figure 3. Kinetic analysis of exchange in **3** by MALDI-TOF mass spectrometry. Exchange in both **3** and **5** (Supporting Information) were monitored by mass spectrometry by integrating the signal from starting material **A** and the appearance of lines corresponding to loss of 1−4 disulfide-linked dansyl groups. The experimental data can be modeled to afford rate constants for the process. See text for details.

with a slope of $\beta = 1$, corresponding to a first-order reaction with respect to the concentration of dansyl groups. Additional data verifying the first-order dependences of [dansyl] and [DTT] on rate for **3** and **5** appear in the Supporting Information.

$$\text{rate} = k_{\text{obs}}[\text{dansyl}]^{\beta} \quad (2)$$

$$\text{rate}_{\text{o}} = k_{\text{obs}}[\text{dansyl}]_{\text{o}}^{\beta} \quad (3)$$

$$\log(\text{rate}_{\text{o}}) = \log(k_{\text{obs}}) + \beta \log[\text{dansyl}]_{\text{o}} \quad (4)$$

Mass Spectrometry. MALDI-TOF mass spectrometry was used to monitor the course of thiol−disulfide exchange for **3** (and **5**, Supporting Information) as indicated in Figure 3 where **A** through **E** correspond to intermediates displaying different numbers of dansyl groups. The spectra are remarkably clean. A detailed picture of the kinetics of the process can be obtained by integrating and normalizing the lines corresponding to loss of one through all four dansyl groups. The results with three representative spectra are shown in Figure 3.

At the beginning of the experiment only **A** displaying all four dansyl-linked chromophores is present, showing a line at MW 4334 Da. Loss of one dansyl group through thiol−disulfide

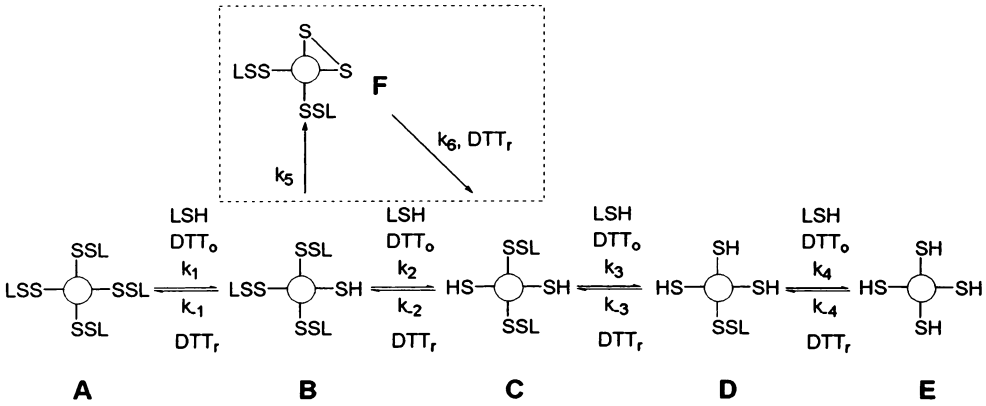

Dendrimer	Constant	$A \Leftrightarrow B$	$B \Leftrightarrow C$	$C \Leftrightarrow D$	$D \Leftrightarrow E$
3	$k_{forward}\,(\times 10^{-4})$	5.66	5.23	5.51	4.52
	$k_{reverse}\,(\times 10^{-2}\,\mathrm{mM})$	3.61	4.55	5.49	1.47
	$K_{eq}\,(\times 10^{-2}\,\mathrm{mM})$	1.56	1.15	1.00	3.07
	$K_{ij}\,(\times 10^{-2}\,\mathrm{mM})$	0.391	0.766	1.51	12.2
5	$k_{forward}\,(\times 10^{-4})$	4.74	8.00	4.27	6.36
	$k_{reverse}\,(\times 10^{-2}\,\mathrm{mM})$	5.29	3.25	1.22	0.22
	$K_{eq}\,(\times 10^{-2}\,\mathrm{mM})$	0.90	2.46	3.50	28.9
	$K_{ij}\,(\times 10^{-2}\,\mathrm{mM})$	0.225	1.64	5.30	116

Figure 4. Simple model linking **A**−**E** by equilibrium processes that involve oxidized and reduced DTT (DTT_o and DTT_r). The processes and intermediate **F** in the dashed boxed are omitted in the simple equilibrium model but are addressed later in the text in a cooperative model.

exchange produces **B** with a peak at MW 4026 Da which increases rapidly before dendrimers displaying two, **C** (MW 3717 Da), and one, **D** (MW 3409 Da), appear after subsequent exchange reactions. The appearance of **E** that has undergone complete exchange to lose all four dansyl groups is indicated by the line at MW 3100 Da. The populations measured reflect contribution of five lines for each species: the major ion, $M + H^+$, its alkali metal adducts $M + Na^+$ and $M + K^+$, and its two major fragmentation products $(M - NH_3)^+$ and $(M - 2NH_3)^+$. Mass resolution supports the existence of dendrimers as poly(thiols) instead of mixtures of thiols and intramolecular (macrocyclic) disulfides. A very similar trend is observed for **5**.

Kinetic Modeling. Modeling a process including potential cooperative (macrocylization) pathways is intractable because of the large number of unknown parameters, including both intermediates and rate constants. Indeed, our attempt to fit rate constants simultaneously to the data using such a scheme yielded estimated parameters of very low statistical significance. As a result, we constructed a minimalist description of the system, four linked species **A**−**E**, and expanded it until the data were adequately described.[39]

Our starting point for the model was the assumption that the intermolecular reactions between dendrimer and DTT_r (forming a more reduced dendrimer, free dansyl group, and oxidized DTT_o) dominated the reaction kinetics. That is, cooperative intramolecular processes carried out within the dendrimer were assumed to contribute insignificantly to the rate of release of dansyl groups. The observed first-order dependence of rate on both dansyl group and DTT_r supports this assumption. The simplest model relating **3** to the species observed by mass spectrometry is shown in Figure 4. While populations **A** and **E** comprise single species, there are four discrete species represented by **B** and **D**, and six discrete species represented by **C**. Populations **A**−**E** can be connected by eight rate expressions (eqs 5−12).[40]

$$r_1 = k_1[\mathbf{A}][\mathrm{DTT_r}] \quad (5)$$

$$r_{-1} = k_{-1}[\mathbf{B}][\mathrm{DTT_o}][\mathrm{LSH}] \quad (6)$$

$$r_2 = k_2[\mathbf{B}][\mathrm{DTT_r}] \quad (7)$$

$$r_{-2} = k_{-2}[\mathbf{C}][\mathrm{DTT_o}][\mathrm{LSH}] \quad (8)$$

$$r_3 = k_3[\mathbf{C}][\mathrm{DTT_r}] \quad (9)$$

$$r_{-3} = k_{-3}[\mathbf{D}][\mathrm{DTT_o}][\mathrm{LSH}] \quad (10)$$

$$r_4 = k_4[\mathbf{D}][\mathrm{DTT_r}] \quad (11)$$

$$r_{-4} = k_{-4}[\mathbf{E}][\mathrm{DTT_o}][\mathrm{LSH}] \quad (12)$$

We initially evaluated the system as a series of unidirectional reactions ($k_{-1} = k_{-2} = k_{-3} = k_{-4} = 0$). The resulting four differential kinetic equations were solved, and the best-fit for the rate constants k_1−k_4 were obtained by using a weighted least-

(39) Maria, G.; Rippin, D. W. T. *Chem. Eng. Sci.* **1993**, *48*, 3855−3864.

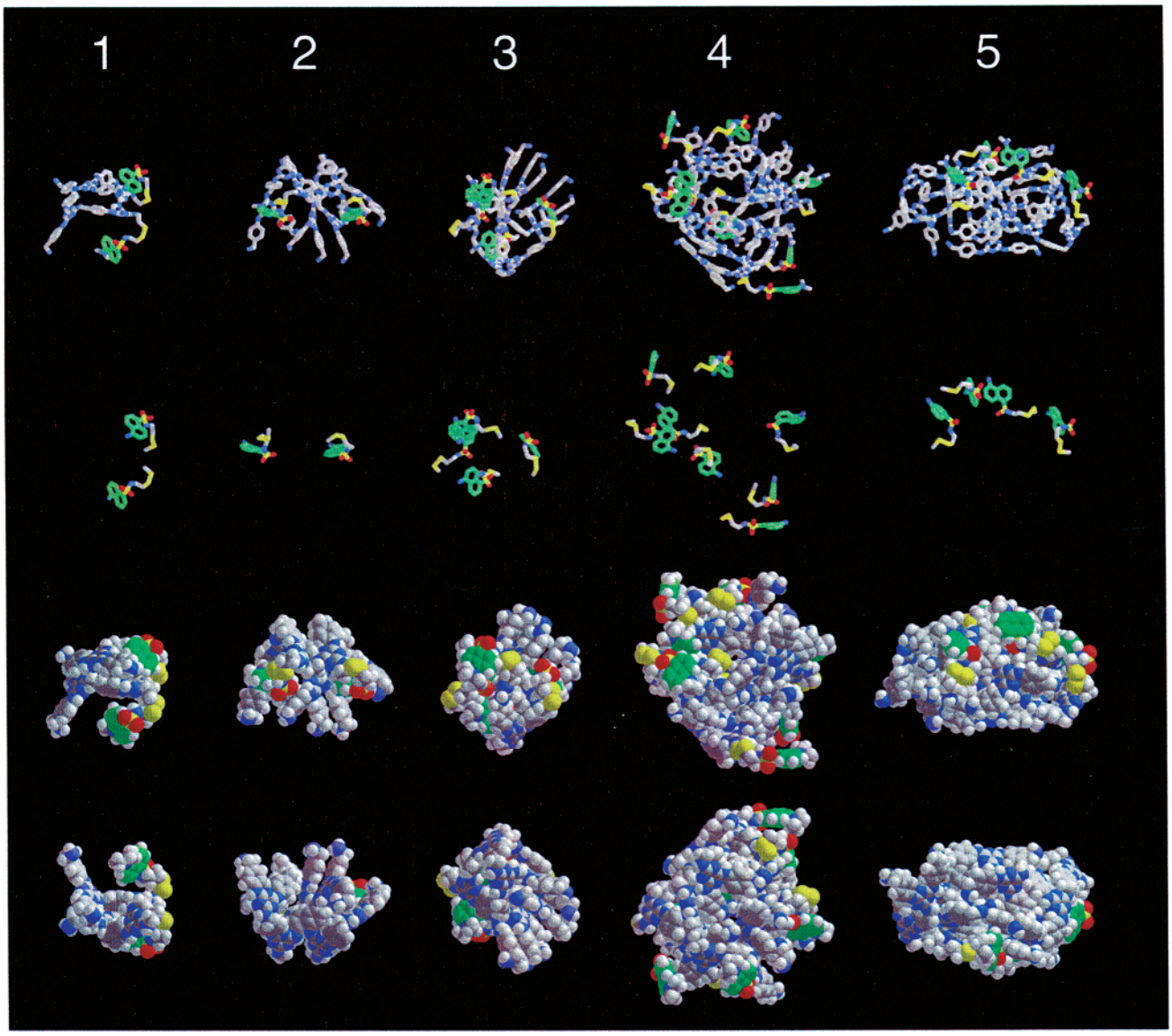

Figure 5. Computational models of **1**−**5**. Representations of **1**−**5** as (top to bottom) wire, wire showing only the dansyl chromophores, and space-filling before and after a 180° rotation.

squares criterion. The model was statistically adequate,[41,42] but deficient because it predicted that [**E**] increases exponentially to ultimately become the only species in solution. This observation neither is realized in the experimental data nor is it consistent with chemical intuition which would suggest that an equilibrium of all species **A**−**E** should be reached. Data from mass spectrometry suggest that the concentration of **E** flattens in time and that an equilibrium likely exists between **A**−**E**.

Consequently, our second model assumed that each step was reversible. We made the simplifying assumption that the reverse reactions were third-order (dendritic thiol, dansyl thiol, and oxidized DTT) although they are actually the sum of at least two reactions. The equations were resolved by using the same weighted least-squares criterion.[43] The best-fit rate constants are shown in Figure 4. The predicted kinetic curves in Figure 3 (solid lines) as well as residual plots and adequacy tests show good agreement between the data and model.[44]

The equilibrium constants for each step of this model, as estimated from the kinetic rate constants, are tabulated in Figure 4. An *apparent* K_{eq} can be calculated by taking the quotient of the forward and reverse rate constants for a step. However, this constant represents the sum of the species denoted with **A**−**E** (**A**:**B**:**C**:**D**:**E** = 1:4:6:4:1).[45] To convert the apparent K_{eq} to the corrected K_{eq} (denoted K_{ij}) which has clearer physical meaning (*vis-à-vis* a single disulfide exchange event linking a single **A**

(40) Throughout all these models, we also assumed that the rate constants associated with these reactions were identical for each dansyl group in dendrimers of the same oxidation state (Supporting Information).
(41) The four reactions model is roughly adequate (i.e., $\chi_c^2 = 32.6 < \chi^2(36 \times 5 - 4; 95\%)$, see Appendix B).
(42) The χ^2 test is a comparison of the predicted model error and the experimental one. The ratio of these errors is validated if it is less than the tabulated χ^2 distribution quantila for a certain assumed confidence level, in this case, 95%. Zwillinger, D. *Standard Mathematical Tables and Formulae*; CRC Press: Boca Raton, 1996.
(43) The residuals for the sum of the squares difference (obsd − exp) of **A**−**E** were assigned weights to more precisely describe **C**, **D**, and **E** such that **A**:**B**:**C**:**D**:**E** = 1:2:10:10:2. Appendix B of the Supporting Information elaborates on this strategy. These adopted weights ensured that fits were equally sensitive to all species residuals (i.e. the difference between the observed and predicted concentrations).
(44) $\chi_c^2 = 32.6 < \chi^2(36 \times 5 - 4; 95\%)$, see Table S2 in Appendix B of the Supporting Information for a description of all the statistical tests.

and **B**, K_{AB}), correction factors of 4, 3/2, 2/3, and 1/4 were applied respectively to K_{eq}'s to yield K_{AB}, K_{BC}, K_{CD}, and K_{DE} based the complete reaction scheme which accounts for individual species of each population (elaborated in the Supporting Information). These constants increase, suggesting that dansyl groups exchange more favorably as the architecture becomes less sterically hindered. Intuitively, we expect the rates of disulfide exchange to be similar for **A**, **B**, **C**, and **D** as these groups of species can adopt a variety of conformations. However, as disulfide groups are lost, the molecular architecture should have more volume accessible to reduced DTT and subsequent reactions, interestingly, for both **3** and **5**.

To determine whether a more extended kinetic scheme incorporating cooperative pathways for release could be statistically supported by the available experimental data, the reversible model was expanded to include macrocyle **F** linked by two additional reactions (eqs 13 and 14, Figure 4, including the dashed box). However, when this expanded system was analyzed as above for **3**, the improvement obtained in adequacy was insignificant, while the parameter statistical tests were negatively affected. Accordingly, we have rejected reactions 13 and 14 and conclude that the eight-reaction model adequately describes the kinetics of the system.

$$r_5 = k_5[\mathbf{B}] \tag{13}$$

$$r_6 = k_6[\mathbf{F}][\mathrm{DTT_r}] \tag{14}$$

Computational Rationalization. Recognizing that the structure of the dendrimer does affect the rate of thiol−disulfide exchange, we turned to computation in an attempt to rationalize these differences. Gas-phase simulations presumably mimic the hydrophobic collapse of these structures. Targets **1**−**5** are shown in Figure 5 as stick models of the full architecture, of only the disulfide-linked chromophores, as space-filling models from the front and back (after a 180° rotation). The radii of gyration calculated for these models (in Å) (**1**−**5**: 7.9, 9.2, 9.8, 16.8, 12.4) are consistent with the hydrodynamic trend observed using GPC of the protected precursors.

Unfortunately, no simple metric for predicting the kinetics of release emerges on the basis of these structures. Instead, and perhaps surprisingly, the best predictor of rate turns out to be the location of the labile bond in the two-dimensional representations shown in Chart 1. The shortcomings of these simulations can be attributed to a number of factors including the large size of these architectures, very few conformational restrictions, a limited pool of target structures to survey, the absence of solvent, and the relative abundance of local minima and relatively large conformational space available for search. Regardless, these computations continue to provide interesting pictures of candidate architectures which serve as excellent mechanisms for challenging our intuition.

(45) The relationship between the full and reduced models is shown in the Supporting Information. The results are that $k_1 = 4k_{AB}$, $k_{-1} = k_{BA}$, $k_2 = 3k_{BC}$, $k_{-2} = 2k_{CB}$, $k_3 = 2k_{CD}$, $k_{-3} = 3k_{DC}$, $k_4 = 4k_{ED}$, $k_{-4} = k_{DE}$. Equilibrium constants describing individual reactions in the full reaction scheme (K_{AB}, K_{BC}, K_{CD}, and K_{DE}) can be related to those obtained by fitting the reduced model to the data (K_{eq}s) with specific corrections described in the text. As required, the product of the K_{eq}s in the reduced system equals that of the full system.

Conclusions

One of our long-term goals for these molecules is their use as models for drug delivery.[46−48] To this end, disulfides could play two roles. First, disulfides might be employed for linking pharmacophores until exposure to cellular concentrations of reductant.[4−6] Second, disulfides could be used to append targeting groups such as peptides[49,50] to direct in a "magic-bullet" sense the dendrimer to specific sites within the body that could complement size-based targeting resulting from the enhanced permeability and retention of tumors for large molecules (the EPR effect).[51−53] The current study shows that both roles remain feasible. Most importantly, dendrimers bearing multiple disulfide-linked hydrophobic groups are tractable and highly water soluble. The opportunity to tailor rates of release as a function of dendrimer structure is very interesting to us (and others, as Takaguchi and co-workers reported thiol−disulfide exchange in a dendrimer with a disulfide core)[54] and may be relevant for delivery regimes that require the dendrimer be internalized by the target cell.

By providing relative populations of the products of thiol−disulfide exchange over time, mass spectrometry provides a description of the kinetics of the process upon which kinetic models can be formulated. The models for both **3** and **5** are tantalizing in that they suggest that the rate of exchange increases as the dendrimer becomes less crowded. The quality of the data and the errors associated with the experiment make such conclusions noteworthy, but preliminary. An additional limitation to these studies merits some comment. While we successfully approached the equilibrium position of **A**−**E** with pure **A**, we have been unsuccessful in purifying **E** by HPLC and reconstituting the reaction mixture. The size and common polarities associated with these dendrimers have made what would be an ordinarily difficult exercise intractable. In conclusion, we add thiol−disulfide-exchange reactions to the list of "dendritic effects" that dendrimers have been shown to impart including catalysis,[55] molecular recognition,[56] cellular uptake,[57] and redox[58] and optical processes.[59]

Acknowledgment. Robert A. Welch Foundation (E.E.S.: A-1439), and the National Institutes of Health (P.A.L.: GM63958; E.E.S.: GM64650) supported these investigations. The Labora-

(46) Liu, M.; Frechet, J. M. J. *Pharm. Sci. Technol. Today* **1999**, *2*, 393−401.
(47) Stiriba, S.-E.; Frey, H.; Haag, R. *Angew. Chem., Int. Ed.* **2002**, *41*, 1329−1334.
(48) Schultz, L. G.; Zimmerman, S. C. *Pharm. News* **1999**, *6*, 25−29.
(49) Pasqualini, R.; Rouslahti, E. *Nature* **1996**, *380*, 364−366.
(50) Arap, W.; Pasqualini, R.; Ruoslhati, E. *Science* **1998**, *279*, 377−380.
(51) Duncan, R.; Pratten, M. K.; Cable, H. C.; Ringsdorf, H.; Llyod, J. B.; *Biochem. J.* **1981**, *196*, 49−55.
(52) Searle, F.; Gac-Breton, S.; Keane, R.; Dimitrijevic, S.; Brocchini, S.; Sausville, E. A.; Duncan, R. *Bioconjugate Chem.* **2001**, *12*, 711−718.
(53) Maeda, H.; Wu, J.; Sawa, T.; Matsumura, Y.; Hori, K. *J. Controlled Release* **2000**, *65*, 271−284.
(54) Takaguchi, Y.; Saito, K.; Suzuki, S.; Hamada, K.; Ohta, K.; Motoyoshiya, J.; Aoyama, H. *Bull. Chem. Soc. Jpn.* **2002**, *75*, 1347−1351.
(55) See, for example: (a) Kleij, A. W.; Gossage, R. A.; Jastrzebski, J. T. B. H.; Boersma, J.; Van Koten, Ge. *Angew. Chem., Int. Ed.* **2000**, *39*, 176−178. (b) Kleij, A. W.; Gossage, R. A.; Klein Gebbink, R. J. M.; Brinkmann, N.; Reijerse, E. J.; Kragl, U.; Lutz, M.; Spek, A. L.; van Koten, G. *J. Am. Chem. Soc.* **2000**, *122*, 12112−12124.
(56) See, for example: (a) Richter-Egger, D. L.; Tesfai, A.; Tucker, S. A. *Anal. Chem.* **2001**, *73* (23), 5743−5751. (b) Koenig, S.; Muller, L.; Smith, D. K. *Chem. Eur. J.* **2001**, *7*, 979−986. (c) Valerio, C.; Ruiz, J.; Fillaut, J.-L.; Astruc, D. *C. R. Acad. Sci.* **1999**, *2*, 79−83. (d) Cardona, C. M.; Alvarez, J.; Kaifer, A. E.; McCarley, T. D.; Pandey, S.; Baker, G. A.; Bonzagni, N. J.; Bright, F. V. *J. Am. Chem. Soc.* **2000**, *122*, 6139−6144.
(57) Wiwattanapatapee, R.; Carreno-Gomez, B.; Malik, N.; Duncan, R. *Pharm. Res.* **2000**, *17*, 991−998.

tory for Biological Mass Spectrometry is a university research facility supported by the Office of the Vice President for Research (TAMU). We thank the Laboratory for Molecular Simulation (TAMU) for providing software and computer time.

Supporting Information Available: Synthesis, modeling, and kinetic data (PDF). This material is available free of charge via the Internet at http://pubs.acs.org.

JA0210906

(58) See, for example: (a) Chow, H.-F.; Chan, I. Y.-K.; Fung, P.-S.; Mong, T. K.-K.; Nongrum, M. F. *Tetrahedron* **2001**, *57*, 1565−1572. (b) Stone D. L.; Smith D. K.; McGrail P. T. *J. Am. Chem. Soc.* **2002**, *124*, 856−864. (c) Astruc, D.; Blais, J.-C.; Cloutet, E.; Djakovitch, L.; Rigaut, S.; Ruiz, J.; Sartor, V.; Valerio, C. *Top. Curr. Chem.* **2000**, *210*, 229−259. (d) Turrin, C.-O.; Chiffre, J.; de Montauzon, D.; Daran, J.-C.; Caminade, A.-M.; Manoury, E.; Balavoine, G.; Majoral, J.-P. *Macromolecules* **2000**, *33*, 7328−7336.

(59) See, for example: (a) Voegtle, F.; Gorka, M.; Hesse, R.; Ceroni, P.; Maestri, M.; Balzani, V. *Photochem. Photobiol. Sci.* **2002**, *1*, 45−51. (b) Jen, A. K.-Y.; Ma, H.; Sassa, T.; Liu, S.; Suresh, S.; Dalton, L. R.; Haller, M. *Proc. SPIE-Int. Soc. Opt. Eng.* **2001**, *4461*, 172−179. (c) Zhu, A.; Bharathi, P.; Drickamer, H. G.; Moore, J. S. *J. Polym. Sci., Part A* **2001**, *39*, 2859−2865.